

Vibrational Analysis of 5'-Methyl-6b,7,9,11a-tetrahydrospiro [chromeno [3', 4': 3,4] pyrrolo [1,2-] thiazole-11,3'-indoline]-2',6(6aH)-dione

S. Pangajavalli¹, R. Ranjithkumar² and S. Ramaswamy³

¹Department of Physics, Sri S. Ramasamy Naidu Memorial College, Sattur, Tamilnadu, (India)

²School of Chemistry, Madurai Kamaraj University, Madurai, Tamilnadu, (India)

³Department of Physics, N.M.S.S. Vellaichamy Nadar College, Madurai, Tamilnadu, (India)

ABSTRACT

Single Crystal of 5'-Methyl-6b,7,9,11a-tetrahydrospiro [chromeno [3', 4': 3,4] pyrrolo [1,2-c] thiazole-11,3'-indoline] -2', 6 (6aH) -Dione was grown and from single crystal XRD, the lattice parameters are $a = 8.365\text{\AA}$, $b = 9.765\text{\AA}$, $c = 11.968\text{\AA}$, $\alpha = 112.62^\circ$, $\beta = 99.39^\circ$, $\gamma = 91.89^\circ$ and it belongs to Triclinic space group P-1. The compound was characterized by FT-IR and Raman analyses. The presence of different functional groups and the nature of their vibrations were identified in experimental vibrational studies through Infra-red and Raman measurements in the range of $4000-400\text{ cm}^{-1}$.

Keywords: FTIR Spectrum, Indoline, Pyrrole, Raman Spectrum, Thiazole.

I. INTRODUCTION

Pyrrole derivatives are well known in many marine organisms [1], some show important bioactivities, such as antitumor activity [2], protein kinase inhibiting activity [3], precursors in porphyrin synthesis [4, 5] and as monomers in polymer chemistry [6], with applications ranging from nonlinear optical materials [7] to electronic noses [8], as selective glycosidase inhibitors, which are used in the treatment of diabetes, cancer, malaria and viral infections, including AIDS [9].

Thiazole and its derivatives are of significant importance in medicinal chemistry as bacterial, herbicidal, fungicidal, antitumor agents [10]. Thiazole derivatives have been used in pharmacological applications, such as antifungal, antiviral, antibacterial, anticancer and anti-inflammatory activities [11]. Thiazole derivatives exhibit diverse biological activities as bacteriostatic, antituberculous and fungistatic agents [12].

Indole derivatives possess biological properties such as antitumor [13], antibacterial and fungicidal [14], anticancer and anti-HIV [15] activities.

Fig.1

II. VIBRATIONAL ANALYSIS

The title compound [C₂₁ H₁₈ N₂ O₃S] belongs to the space group P-1 and has a triclinic symmetry with two formula units per cell. The factor group analysis using the standard correlation method was carried out. Excluding the acoustic modes, 267 normal modes are predicted. These genuine modes can be decomposed into the irreducible representations of the factor group C_i as $\Gamma = 135A_g^R + 132A_u^{IR}$ (Table 1), where A_g species are Raman active and A_u species are infrared active. The observed infrared spectrum of the title compound in the spectral range between 4000 and 400 cm⁻¹ is presented in Fig.2 and the corresponding Raman spectrum in the spectral range between 4000 and 70 cm⁻¹ is depicted in Fig.3 The observed vibrational bands in the infrared and Raman spectra with their corresponding assignments are tabulated in Table 2. The molecular structure has various functional groups such as carbonyl, hydroxyl, CH₃, CH₂, C-H, C-C=O, C-N, C=O, N-H, C-S and monosubstituted benzene ring. The high wavenumber region around 3800-1500cm⁻¹ consists the bands due to N-H, O-H, CH, CH₂ and C-N stretching vibrations. The low wavenumber region around 1500-450 cm⁻¹ contains bands due to deformation vibrations of the various groups. The lattice vibration modes occur below 450 cm⁻¹.

Table 1

Factor group analysis of the title compound, C₂₁H₁₈N₂O₃S
Crystal space group: P-1 = C_i; Z=2; Z^B=2

Degrees of freedom for each species	Molecular symmetry species	Modes and Site symmetry species C ₁	Factor group species C _i
C ₂₁ H ₁₈ N ₂ O ₃ S	Vibrational	A	135A _g 132A _u
270			

$$\Gamma_{cryst}^{total} = 135A_g^R + 135A_u^{IR}$$

$$\Gamma_{cryst}^{int} = \Gamma_{cryst}^{total} - \Gamma_{acoustic} = 135A_g + 135A_u - (3A_u)$$

$$\Gamma_{cryst}^{int} = 135A_g^R + 132A_u^{IR}$$

The notation proposed by Wilson¹² will be used throughout this paper for assigning the wavenumbers to the vibrational bands in the spectra.

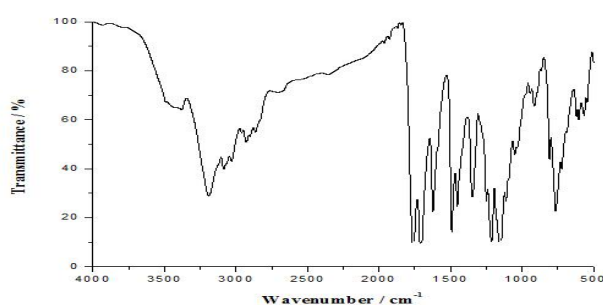


Fig.2 Infra-red spectrum

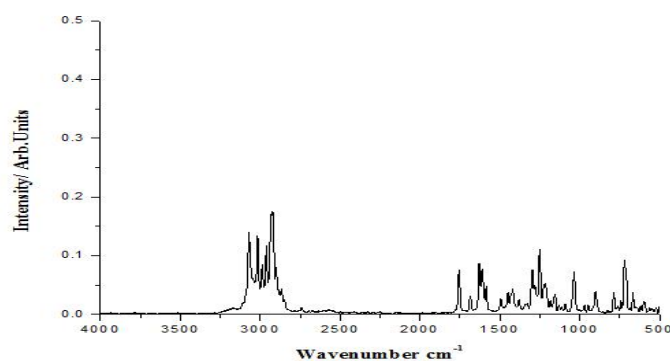


Fig3. Raman spectrum

2.1 Monosubstituted Benzene Ring Vibrations

The wave numbers of the aromatic C-H stretching vibrations in monosubstituted benzenes fall in the range 3100 - 3000 cm^{-1} [33,35,36,44,45]. In the infrared spectrum one medium band at 3086 and one weak band at 3030 cm^{-1} , whereas in the Raman Spectrum two strong bands at 3070 and 3017 cm^{-1} are assigned to aromatic C-H stretching vibrations.

In the substituted benzenes, the vibrations in the region 1600 – 1500 cm^{-1} mainly involve quadrant stretching of the ring C=C bonds. But there is a little interaction with CH in plane bending [33, 42]. In the present investigation, the strong band at 1490 cm^{-1} in FTIR, the bands at 1493 cm^{-1} , 1586 cm^{-1} and 1612 cm^{-1} in Raman spectra are due to quadrant ring stretching components.

The Semi-circle ring stretching vibrations mix strongly with C-H in-plane bending vibrations and split into two components (ν_{19a} and ν_{19b}) in substituted benzenes. The first component (ν_{19a}), involving Semi-circle ring stretching mixed with C-H bending, usually appears at 1510- 1470 cm^{-1} for monosubstituted benzenes [33, 42]. The infrared intensity is strong for electron donor groups and weak or absent when these are not present. The Raman intensity is usually weak. In the crystal under study, this mode appears as a strong band at 1490 cm^{-1} in FTIR and a weak band (1493 cm^{-1}) in the Raman spectrum. The second component involving semi circle stretching mixed with C-H bending appears at 1465 – 1430 cm^{-1} for monosubstituted benzenes [33, 42]. The infrared intensity of this component is relatively independent of the nature of the substituent. The Raman intensity is usually weak. The strong band at 1452 cm^{-1} in the infrared spectrum and the corresponding weak intensity Raman bands at 1451 cm^{-1} , 1419 cm^{-1} are due to this component.

In-plane C-H deformation mode (ν_{18b}) falls in the range 1082-1065 cm^{-1} and is very weak in intensity in both the infrared and Raman spectra [33, 43]. In the present investigation, the weak bands at 1051 cm^{-1} in FTIR and at 1091 cm^{-1} in Raman spectrum are assigned to in-plane C-H deformation mode (ν_{18b}).

In monosubstituted benzene, a Raman band of medium intensity at 1160 - 1150 cm^{-1} appears due to the in-plane C-H deformation mode (ν_{15}) [33,43]. A medium intensity Raman band at 1155 cm^{-1} is attributed to the in-plane C-H deformation ν_{15} mode. As this mode is overlapped by C-N-H stretching and C-S stretching vibrations, the corresponding band in the infrared spectrum appears strong at 1153 cm^{-1} . Another in-plane C-H deformation mode (ν_3) is expected to appear in the region 1330-1250 cm^{-1} and is very weak in both infrared and Raman

spectra in monosubstituted benzenes [33, 43]. For the compound under study, the weak band at 1248cm^{-1} in the infrared spectrum and the corresponding band at 1251cm^{-1} in Raman spectrum appears as a very strong band instead of a very weak band due to the overlapping of in-plane C-H deformation vibrations are attributed ν_3 mode.

For monosubstituted benzene, the out-of-plane quadrant deformation mode (ν_{16a}) is either forbidden or very weak in the infrared spectrum and is also a very weak band in the Raman spectrum at $420\text{-}390\text{cm}^{-1}$ [33,43]. This mode ν_{16a} is forbidden in both infrared and Raman spectra. The other quadrant deformation mode (ν_{16b}) generally occurs in the range $560\text{-}430\text{cm}^{-1}$ and is weak in the Raman spectrum. This mode is observed as a strong band at 488cm^{-1} in the infrared spectrum and as a weak band at 499cm^{-1} in the Raman spectrum.

For monosubstituted benzene, the out-of-plane C-H deformation mode (ν_5) gives rise to a Raman band of sufficient intensity. This mode usually occurs in the region $1000\text{-}970\text{cm}^{-1}$ and appears as a shoulder on the low wavenumber side of the intense band at 1000cm^{-1} due to the trigonal ring 'breathing' mode (ν_{12}) [43]. The weak intensity band at 970cm^{-1} in the Raman spectrum are assigned to out-of-plane C-H deformation mode (ν_5).

The in-phase, out-of-plane aromatic C-H wag vibrations give rise to strong infrared bands and they appear in the spectrum in different regions according to the number of adjacent hydrogen atoms in the benzene ring. For monosubstituted benzenes, with five or four adjacent hydrogen atoms in this band falls in the region $805\text{-}728\text{cm}^{-1}$ [33, 42]. The strong band at 765cm^{-1} in the infrared spectrum and the corresponding weak Raman band at 742cm^{-1} are attributed to the in-phase, out-of-plane aromatic C-H wag vibrations.

2.2 Pyrrole Ring Vibrations

In the present investigation, the C-H stretching vibrations of pyrrole ring occur as a strong, broad band at 3188cm^{-1} in the infrared spectrum. Due to the overlapping of C-H stretching vibrations of the pyrrole ring with the N-H stretching vibrations of thiazole ring, a broad band instead of the sharp peak appears in the infrared spectrum [42]. Symmetric stretching vibrations (pyr. half-ring) in the pyrrole ring appears at 1347cm^{-1} and 1382cm^{-1} [41] in the infrared and Raman spectrum respectively. Stretching vibrations (pyr. quarter-ring) are attributed at 1329cm^{-1} [41] in the Raman spectrum. Absorbance at 1111cm^{-1} and 1051cm^{-1} [41] in the infrared spectrum and corresponding absorbance at 1091cm^{-1} [41] in the Raman spectrum is attributed to stretching vibrations (pyr. breathing) of the pyrrolering. N-H wagging mode of pyrrole is observed at 765cm^{-1} and 788cm^{-1} [37,39] in the infrared and Raman spectrum respectively. The weak intensity band at 619cm^{-1} in the Raman spectrum is assigned to out-of-plane deformation of pyrrole rings [41]

2.3. Carbonyl Vibrations

For the crystal under study, the weak band at 3378cm^{-1} in the FTIR spectrum is assigned to C=O overtone [44]. A very strong band at 1760cm^{-1} in the infrared and a strong band at 1756cm^{-1} in the Raman spectrum [16,38,42] are assigned to C=O stretching vibrations in five membered rings. Stretching vibrations of C=O in the six membered rings are observed as a very strong band at 1707cm^{-1} in FTIR and medium intensity band at 1685cm^{-1} in the Raman spectrum [16,38,45]. Intramolecular hydrogen bonded C=O stretching appears as strong bands at 1622cm^{-1} and 1630cm^{-1} in the FTIR and Raman spectrum [44] respectively. The C=O in-plane bending and the out-of-plane bending vibrations are expected in the regions $725\pm 70\text{cm}^{-1}$ and $540\pm 80\text{cm}^{-1}$

www.ijates.com

respectively [17]. In the title compound, the in-plane bending vibrations are identified at 765 cm^{-1} in the FTIR and at 722 cm^{-1} in the Raman spectrum. The out-of-plane bending vibrations are observed at 488 cm^{-1} in the FTIR and the corresponding band at 499 cm^{-1} in the Raman spectrum. The in-plane out-of-phase C=O vibrations are observed at 369 cm^{-1} in the Raman spectrum [16].

2.4. Thiazole Ring Vibrations

In the title compound, the N-H stretching vibrations appear as strong band at 3188 cm^{-1} in the FTIR spectrum [20,31]. The medium intensity band at 3086 cm^{-1} and the weak band at in the FTIR are attributed to C-H stretching vibrations of the thiazole ring [22,31]. The N-H bending vibrations occur as a very strong band at 1490 cm^{-1} in the FTIR and the weak band at 1493 cm^{-1} in the Raman spectrum [22]. The strong band at 1452 cm^{-1} in the FTIR and the corresponding weak band at 1451 cm^{-1} are identified as C-C_{phenyl} bending vibrations [22]. Due to the overlapping of C-N-H and C-S stretching vibrations, a very strong broad band appears at 1153 cm^{-1} in the FTIR and the corresponding weak band at 1155 cm^{-1} in the Raman spectrum [22]. The weak bands at 942 cm^{-1} and 947 cm^{-1} in the FTIR and Raman spectrum respectively are identified as N-H wagging [22]. The C-S stretching vibrations occur at 619 cm^{-1} in both FTIR and Raman spectrum [23]. The weak band at 545 cm^{-1} is assigned to in-plane C-S-C bending [23].

2.5. Indole Ring Vibrations

In the present investigation, the bands at 1452 cm^{-1} , 1248 cm^{-1} , 1111 cm^{-1} are attributed to in-plane N-H bending vibrations [28,29,30]. The out-of-plane C-H bending occurs at 942 cm^{-1} in the FTIR and at 947 cm^{-1} in the Raman spectrum [29]. The band at 619 cm^{-1} in both FTIR and Raman spectrum are assigned to out-of-plane N-H bending vibrations [29]. The out-of-plane N-H bending vibrations appear at 565 cm^{-1} , 545 cm^{-1} in the FTIR and at 563 cm^{-1} in the Raman spectrum [28,29].

2.6. CH₃ Vibrations

For the crystal under study, the weak band at 2960 cm^{-1} and the medium band at 2928 cm^{-1} in the FTIR and the corresponding strong bands at 2963 cm^{-1} and 2922 cm^{-1} are observed as antisymmetric (CH₃) stretching vibrations [16]. The symmetric C-H vibrations (CH₃) are identified at 2864 cm^{-1} in the FTIR and at 2868 cm^{-1} and 2741 cm^{-1} in the Raman spectrum [16]. The strong band at 1452 cm^{-1} and the corresponding weak band at 1451 cm^{-1} in the FTIR and the weak band at 1382 cm^{-1} are assigned to antisymmetric deformation of CH₃ [16]. CH₃ rocking appears at 1051 cm^{-1} in the FTIR and 1091 cm^{-1} in the Raman spectrum [16].

2.7. CH₂ Vibrations

The medium intensity band at 3086 cm^{-1} and weak band at 3030 cm^{-1} in the IR and the corresponding strong bands at 3070 and 3017 cm^{-1} in the Raman indicate the presence of the CH₂ asymmetric stretching vibration [16, 34, 38, 39, 41, 42]. The CH₂ symmetric stretching vibration appears as a weak band at 2960 cm^{-1} and the medium intensity band at 2928 cm^{-1} in the IR and strong bands at 2963 cm^{-1} and 2922 cm^{-1} in the Raman spectrum. The strong peak at 1452 cm^{-1} and the weak band at 1451 cm^{-1} [34, 42] in the infrared and Raman spectra respectively are attributed to the CH₂ deformation vibrations. The CH₂ twisting vibrations in CH₂ chains

occur at 1051 cm^{-1} in the FTIR and at 1329 cm^{-1} in the Raman spectrum. The CH_2 scissoring, wag and twist vibrations have also been identified and assigned.

2.8. C-N Vibrations

In the title compound, the bands at 1347 cm^{-1} , 1213 cm^{-1} , 1111 cm^{-1} and at 1216 cm^{-1} , 1091 cm^{-1} , 1035 cm^{-1} are attributed to C-N stretching vibrations in the infrared and Raman spectrum [26,34,35,44] respectively. The weak intensity bands at 354 and 369 cm^{-1} in the Raman spectrum are assigned to C-N-C skeletal deformations [43].

Table 2

Infrared ($\bar{\nu}/\text{cm}^{-1}$)	Raman ($\bar{\nu}/\text{cm}^{-1}$)	Assignment
3378 (w)		$\nu\text{C}=\text{O}$ overtone
3188 (s, br)		$\nu\text{N}-\text{H}_{\text{thiazole}} + \nu\text{C}-\text{H}_{\text{pyrrole}}$
3086 (m)	3070(vs)	$\nu\text{C}-\text{H}_{\text{thiazole}} + \nu_{\text{as}}\text{C}-\text{H}$ of $\text{CH}_2 + \nu\text{C}-\text{H}_{\phi} + \text{ar C}-\text{H}$ ν
3030 (w)	3017 (vs)	$\nu_{\text{s}}\text{C}-\text{H}_{\text{thiazole}} + \nu_{\text{as}}\text{C}-\text{H}$ of $\text{CH}_2 + \nu\text{C}-\text{H}_{\phi} + \text{ar C}-\text{H}$ ν
2960 (w)	2963 (s)	$\nu_{\text{as}}\text{C}-\text{H}$ of $\text{CH}_3 + \nu_{\text{s}}\text{C}-\text{H}$ of CH_2
2928 (m)	2922 (vs)	$\nu_{\text{as}}\text{C}-\text{H}$ of $\text{CH}_3 + \nu_{\text{s}}\text{C}-\text{H}$ of CH_2
2864 (w)	2868 (w)	$\nu_{\text{s}}\text{C}-\text{H}$ of CH_3
	2741 (w)	$\nu_{\text{s}}\text{C}-\text{H}$ of CH_3
1926		Overtone of indole ring
1760 (vs)	1756 (s)	$\nu\text{C}=\text{O}$ Fermi resonance doublet
1707 (vs)	1685 (m)	$\nu\text{C}=\text{O}$
1622 (s)	1630 (s)	$\text{C}=\text{O}$ intramolecular hydrogen bond + $\nu\text{C}-\text{C}_{\phi} + \delta\text{N}-\text{H}$
	1612 (s)	$\delta\text{N}-\text{H} + \nu$ quad. ring
	1586 (m)	ν quad. ring
1490 (vs)	1493 (w)	$\delta_{\text{as}}\text{C}-\text{H}$ of $\text{CH}_3 + \text{N}-\text{H}_{\text{thiazole}}$ bend + $\alpha\text{CH}_2 + \nu$ s.c.ring(ν_{19a}) + ν quad. ring
1452 (s)	1451 (w)	$\alpha\text{CH}_2 + \text{def}$ of $\text{CH}_3 + \text{C}-\text{C}_{\phi}$ bend + Indole skeletal vibrations + $\delta\text{N}-\text{H} + \alpha\text{CH}_3 + \nu$ s.c.ring(ν_{19b})
	1419 (w)	ν s.c.ring(ν_{19b})
	1382 (w)	as .def. of $\text{CH}_3 + \nu_{\text{s}}$ (pyr.half-ring)
1347 (s, br)		$\omega\text{CH}_2 + \nu\text{C}-\text{N} + \alpha\text{CH}_3 + \nu_{\text{s}}$ (pyr.half-ring)
	1329 (w)	$\tau\text{CH}_2 + \nu$ (pyr. quarter-ring) + $\phi\delta\text{CH}$ def. (ν_3)
	1298 (s)	ωCH_2
1248 (w)	1251 (vs)	$\delta\text{C}-\text{H} + \phi\delta\text{CH}$ def. (ν_3)
1213 (vs, br)	1216 (m)	$\delta\text{C}-\text{H} + \nu\text{C}-\text{N}$
1153 (vs, br)	1155 (m)	$\delta\text{C}-\text{H} + \nu\text{C}-\text{N}-\text{H} + \nu\text{C}-\text{S} + \phi\delta\text{CH}$ def. (ν_{15})
1111 (w)		$r\text{CH}_3 + \delta\text{C}-\text{H} + \nu\text{C}-\text{N} + \text{N}-\text{H}$ bending + ν (pyr. breathing)
	1091 (w)	$r\text{CH}_3 + \delta\text{C}-\text{H} + \nu\text{C}-\text{N} + \text{N}-\text{H}$ bending + ν (pyr. breathing) + $\phi\delta\text{CH}$ def. (ν_{18b})S
1051 (w)		$\tau\text{CH}_2 + r\text{CH}_3 + \delta\text{C}-\text{H} + \nu\text{C}-\text{N} + \nu$ (pyr. breathing) + $\phi\delta\text{CH}$ def. (ν_{18b})
	1035 (s)	$\nu\text{C}-\text{N}$
	970 (w)	$\phi\pi\text{CH}$ def. (ν_5)
942 (w)	947 (w)	$\pi\text{C}-\text{H} + \omega\text{N}-\text{H} + \text{indole skeletal vibrations} + \pi\text{C}-\text{H}$
914 (m)	901 (m)	$\pi\text{C}-\text{H} + r\text{CH}$
807 (m)		$\pi\text{C}-\text{H} + \delta\text{C}-\text{H} + \pi=\text{CH} + \text{ar CH} + \nu\text{S}-\text{C}$
	788 (m)	Pyr. N-H ω
765 (s, br)		$\delta\text{C}-\text{C}-\text{C} + \delta\text{C}-\text{H} + \pi$ indol phenyl ring + In -phase π

		CH(ring) ω +pyr.N-H ω +, δ C=O
	742 (w)	In -phase π CH (ring) ω
722 (w)	722 (vs)	r CH ₂ + δ C-C-C+ indole skeletal vibrations+ δ O-C-O+ ν S-C-N + δ C=O
619 (w)	619 (w)	ν C-S + δ S-C-N + π N-H + π pyr.def. ϕ o.p. Sextant ring def. (ν_4)
565 (m)	563 (w)	π N-H+ π S-C-N o.p.def.ofpyr
545 (w)		δ C-S-C + π N-H+ π S-C-N
	499 (w)	ϕ π quad. def. (ν_{16b}) + π C=O
488 (s)		π N-H+ C-N-C skeletal def.+Carbonyl π def.+ ϕ π quad. def. (ν_{16b}) + π C=O
	431 (vs)	i.p.C-C(=O)-C def.
	369 (w)	π CCC+C-N-C skeletal def.
	354 (w)	δ C=O+ C-N-C skeletal def.
	332 (w)	δ CCC+ Torsion C-C
	283 (s)	α CH ₂ + Torsion C-C
	225 (m)	Torsion CH ₃
	195 (vs)	δ CCO
	160 (w)	π CNCH
	118 (vs)	π CNCH
	97 (vs)	Torsion C-C
	83 (vs)	Torsion C-C

ar - aromatic, ν - stretching, as- antisymmetric stretching, s - symmetric stretching, def. - deformation, δ - bending in-plane, π - bending out-of-plane, quad-quadrant, ϕ - phenyl ring, pyr - pyrrole ring, s.c. - Semi-circle α - scissoring, ω - wagging, τ - twisting, r - rocking.

III CONCLUSION

The compound, 5'-Methyl-6b, 7, 9,11a- tetrahydrospiro [chromeno [3', 4': 3, 4] pyrrolo [1, 2-] thiazole-11,3'-indoline] -2', 6 (6aH) -dione was mainly used in biological activities suchas antitumor and anticancer agents. The compound was investigated experimentally by FTIR and Raman vibrational spectroscopic methods. Various functional groups were confirmed by FTIR and Raman spectrum.

REFERENCES

- [1] D. D. Li, G. H. Tang, X. C. Zeng, X. Y. Xu and G. Huang, 1-Ethyl-1H,6H-pyrrolo[2,3-c]azepine-4,8(5H,7H)-dione,E65,2009,o1928.
- [2] M. G. Banwell, E. Hamel, D. C. R. Hockless, P. VerdierPinard, A. C Willis and D. J. Wong,4,5-Diaryl-1H-pyrrole-2-carboxylates as combretastatin A-4/lamellarin T hybrids: Synthesis and evaluation as anti-mitotic and cytotoxic agents, *Bioorg. Med. Chem.*, 14, 2006, 4627-4638.
- [3] A. C. B. Sosa, K. Yakushijin and D.A. Horne.,Synthesis of Axinohydantoin, *J. Org. Chem.*, 67, 2002., 4498- 4500.
- [4] A. J. F. N. Sobral&A. M. D. A. RochaGonsalves,The manganese complex of 2, 3, 7, 8, 12, 13, 17, 18-octaphenylporphyrin as epoxidation catalyst, *J. PorphyrinsPhthalocyanines*, 5, 2001a, 428-430.
- [5] A. J. F. N. Sobral and A. M. D. A. RochaGonsalves,5, 15-Diaryl- β -substituted-porphyrinato-manganese (III) chlorides as probes for structure-activity relationships in porphyrin-based epoxidation catalysts, *J. PorphyrinsPhthalocyanines*, 5, 2001b, 861-866.



- [6] T. W. Brockmann and J. M. Tour, Synthesis and Properties of Low-Bandgap Zwitterionic and Planar Conjugated Pyrrole-Derived Polymeric Sensors. Reversible Optical Absorption Maxima from the UV to the Near-IR, *J. Am. Chem. Soc.*, *117*, 1995, 4437-4447.
- [7] K. S. Suslick, C. T. Chen J. G. . Mer. dith and L. T. Cheng, Push-pull porphyrins as nonlinear optical materials, *J. Am. Chem. Soc.*, *114*, 1992, 6928-6930.,
- [8] C. DiNatale, R. Paolesse, A. Macagnano, A. Mantini, C. Goletti, E. Tarizzo and A. Amico, Characterization and design of porphyrins-based broad selectivity chemical sensors for electronic nose applications, *Sens. Actuators, B*, *52* (1), 1998., 162-168.
- [9] A. Kilonda, F. Compennolle, and G. J. Hoornaert, Synthesis of 2-azido-6-amino and 2-fluoro-6-amino analogs of 1-deoxynojirimycin, *J. Org. Chem.*, *60*, 1995, 5820-5824.
- [10] N. Sivakumar, V. Viswanathan, J. N. S. Rao, R. Raghunathan and D. Velmurugan, Crystal structure of 6-(4-chlorophenyl)-6a-nitro-6,6a,6b,7,9,11a-hexahydrospiro[chromeno[3',4':3,4]pyrrolo[1,2-c]thiazole-11,11'-inde) o[1,2-b]quinoxaline] chloroform monosolvate, *E70*, 2014, o1111-1112.
- [11] V. S. Shruthy and Y. Shakkeela, Int., In Silico Design, Docking, Synthesis And Evaluation Of Thiazole Schiff Bases, *J. Pharm Pharm Sci.*, *6*, 2014, 271-275.
- [12] L. Shao, Z. Jin, J.-B. Liu, X. Zhou, Q. Zhang, Y. Hu and J.-X. Fang, 2-Amino-4-(2,5-dichlorophenyl)-5-(1H-1,2,4-triazol-1-yl)-1,3-thiazole, *Acta Cryst.*, *E60*, 2004, o2517-o2519.
- [13] N. I. Ziedan, F. Stefanelli, S. Fogli and A. D. Westwell, Design, synthesis and pro-apoptotic antitumor properties of indole-based 3,5-disubstituted oxadiazoles, *Eur. J. Med. Chem.*, *45*, 2010, 4523-4530.
- [14] K. C. Joshi and P. Chand, Biologically active indole derivatives, *Pharmazie*, *37*, 1982, 1-12.
- [15] E. Pomarnackam and I. Kozlarska-Kedra, Synthesis of 1-(6-chloro-1,1-dioxo-1,4,2-benzodithiazin-3-yl) semi-carbazides and their transformation into 4-chloro-2-mercapto-N-(4,5-dihydro-5-oxo-4-phenyl-1H-1,2,4-triazol-3-yl) benzenesulfonamides as potential anticancer and anti-HIV agents, *Farmaco*, *58*, 2003, 423-429.
- [16] M. A. Al-Alshaikh, O. A. Al-Deeb, N. Z. Alzoman, A. A. El-Emam, R. Srivastava, A. K. Sachan, O. Prasad and L. Sinha, Spectroscopic and electronic structure calculation of a potential chemotherapeutic agent 5-propyl-6-(p-tolylsulfanyl) pyrimidine-2,4 (1H, 3H) -dione using first principles, *J. molstruc*, *1100*, 2015, 225-236.
- [17] M.S. Boobalan, S. Ramalingam, M. Amaladasan, D. Tamilvendan, G. Venkatesa Prabhu and M. Bououdina, A computational perspective on equilibrium geometry, vibrational spectra and electronic structure of antioxidant active Mannich Base - 1-[(pyridin-2-yl amino methyl] pyrrolidine-2,5-dione, *J. molstruc*, *1072*, 2014, 153-172.
- [18] F.A.M. Al-Omary, Y. Sheena Mary, S. Beegum, C. Yohannan Panicker, M.M. Al-Shehri, A. A. El-Emam, S. Armaković, Sanja J. Armaković and C. V. Alsenoy, Molecular conformational analysis, reactivity, vibrational spectral analysis and molecular dynamics and docking studies of 6-chloro-5-isopropylpyrimidine-2,4 (1H,3H) -dione, a potential precursor to bioactive agent, *J. molstruc*, *1127*, 2017, 427-436.

- [19] G. Y. Nagesh and B.H.M. Mruthyunjayaswamy, Synthesis, characterization and biological relevance of some metal (II) complexes with oxygen, nitrogen and oxygen (ONO) donor Schiff base ligand derived from thiazole and 2-hydroxy-1-naphthaldehyde, *J.molstruc*, 1085,2015,198-206.
- [20] G.Y.Nagesh, K. Mahendra Raj and B.H.M. Mruthyunjayaswamy, Synthesis, characterization, thermal study and biological evaluation of Cu(II), Co(II), Ni(II) and Zn(II) complexes of Schiff base ligand containing thiazole moiety, *J.mol (truc*, 1079, (015,423-432.
- [21] F. Sen, O. Ekici, M. Dincer and A. Cukurovali, J. omparati, e study on 4-(4-(3-mesityl-3-methylcyclobutyl)thiazole-2-yl) -1-thia-4-azaspiro [4.5] decan-3-one: Experimental and density functional methods, *J. molstruc*, 1086,2015,109-117.
- [22] R. Anbazhagan and K.R. Sankaran, Syntheses, spectral characterization, single crystal X-ray diffraction and DFT computational studies of novel thiazole derivatives, *J. molstruc*, 1050,2013,73-80.
- [23] V. Arjunan, P.S. Balamourougane, C.V. Mythili, S. Mohan and V. Nandhakumar, Vibrational, nuclear magnetic resonance and electronic spectra, quantumchemical investigations of 2-amino-6-fluorobenzothiazole, *J. molstruc*, 1006,2011,247-258.
- [24] A. Dylong, W. Goldeman, M. Sowa, K. Slepokura, P. Drozdowski and E. Matczak-Jon, Synthesis, crystal structures and spectral characterization of imidazo [1,2-a] pyrimidin-2-yl-acetic acid and related analog with imidazo [2,1-b] thiazole ring, *J. molstruc*, 1117,2016,153-163.
- [25] O. F. V. Vuelas, J.V. H. Madrigal, R. Gavino, M. A. Tlenkopatchev, D. M. Morales, J.M. G. Acacio, Z. G. Sandoval, C. GMorales, A. A. Castolo and A. P. Contreras, X-ray, DFT, FTIR and NMR structural study of 2, 3-dihydro-2-(R-phenylacylidene)-1, 3, 3-trimethyl-1H-indole, *J.molstruc*, 987, 2011, 106-118.
- [26] B. M. Ociepa, X-ray diffraction and vibrational spectroscopic studies of indolecarboxylic acids and their metal complexes: Part VII. Indole-2-carboxylic acid and catena-poly [(diaquazinc (II))-bis (μ^2 -indole-2-carboxylato-O: O')], *J.VibSpec*, 49, 2009, 68-79.
- [27] Ru Sun, Jianlin Yao, Shujin Li and Renao Gu, Raman spectroscopic and density functional theory studies on a benzothiazole-2-thione derivative, *J. VibSpec.*, 47, 2008, 38-43.
- [28] B. M. Ociepa and E.R. Sokolowska, X-ray and infrared spectrum on metal complexes with indolecarboxylic acids Part V. Catena-poly [{aqua (η^2 -indole-3-propionato-O, O0) zinc } - η^2 - μ -indole-3-propionato-O, O0:-O], *J.VibSpec*, 43, 2007, 405-414.
- [29] B. M. Ociepa and B. Marciniak, X-ray and vibrational spectra on metal complexes with indolecarboxylic acids Part IV. Catena-poly [{aqua (η^2 -indole-3-carboxylato-O, O0) zinc } - μ -indole-3-carboxylato-O: O0], *J.VibSpec.*, 43, 2007, 297-305.
- [30] B. M. Ociepa, X-ray diffraction and vibrational spectroscopic studies of indolecarboxylic acids and their metal complexes Part VI. Indole-3-propionic acid and catena-poly [(di- μ^3 -aqua) (η^2 - : - (μ^2 -indole-3-propionato-O, O0:-O) (μ^3 -indole-3-propionato-O) disodium], *J.VibSpec.*, 46, 2008, 115-127.
- [31] F. Sen, M. Dincer and A. Cukurovali, Synthesis, spectroscopic characterization and quantum chemical computational studies on 4-(3-methyl-3-phenylcyclobutyl) -2-(2- undecylidenehydrazinyl)thiazole, *J. molstruc*, 1076, 2014, 1-9.



- [32] F. Sen, M. Dincer, A. Cukurovalı and I. Yılmaz, N-[4-(3-methyl-3-mesityl-cyclobutyl) -thiazol-2-yl] - succinamic acid: X-ray structure, spectroscopic characterization and quantum chemical computational studies, *J. molstruc*, 1046, 2013, 1–8.
- [33] S. Ramaswamy, R. K. Rajaram and V. Ramakrishnan, Raman and IR spectral studies of D-phenylglycinium perchlorate, *J. Raman Spectrosc.*, 33, 2002, 689-698.
- [34] S. Ramaswamy, R. K. Rajaram and V. Ramakrishnan, Vibrational spectra of bis (L-ornithinium) chloride nitrate sulfate, *J. Raman Spectrosc.*, 36, 2005, 12-17.
- [35] R. Anitha, S. Athimoolam, M. Gunasekaran and K. Anitha, X-ray, vibrational spectra and quantum chemical studies on a new semiorganic crystal: 4-Chloroanilinium perchlorate, *J. Mol. Struc.*, 1076, 2014, 115-125.
- [36] S. Thangarasu, S. Sureshkumar, S. Athimoolam, B. Sridhar, S. AsathBahadur, R. Shanmugam and A. Thamarichelvan, Synthesis, structure, spectral, thermal analyses and DFT calculation of a hydrogen bonded crystal: 2-Aminopyrimidinium dihydrogenphosphate monohydrate, *J. Mol. Struc.*, 1074, 2014, 107-117.
- [37] P. Rawat, R. N. Singh, Spectral analysis, structural elucidation, and evaluation of both nonlinear optical properties and chemical reactivity of a newly synthesized ethyl-3,5-dimethyl-4-[(toluenesulfonyl) -hydrazonomethyl] -1H-pyrrole-2-carboxylate through experimental studies and quantum chemical calculations, *J. Mol. Struc*, 1054-1055, 2013, 65–75.
- [38] P. Rawat, R. N. Singh, Evaluation of molecular assembly, spectroscopic interpretation, intra-/inter molecular hydrogen bonding and chemical reactivity of two pyrrole precursors, *J. Mol. Struc*, 1075, 2014, 462–470.
- [39] P. Rawat, R. N. Singh, Spectral analysis, structural elucidation and evaluation of chemical reactivity of synthesized ethyl-4-[(2-cyano-acetyl) -hydrazonomethyl] -3,5-dimethyl-1H-pyrrole-2-carboxylate through experimental studies and quantum chemical calculations, *J. Mol. Struc*, 1074, 2014, 201-212.
- [40] P. Rawat, R.N. Singh, Vikas Baboo, Priyadarshni Niranjana, Himanshu Rani, Rajat Saxena, Sartaj Ahmad, synthesis, spectroscopic analysis and theoretical study of new pyrrole-isoxazolines derivative, *J. Mol. Struc*, 1129, 2016, 37-49.
- [41] Wei Li., Yibo Wang., Lanying Yang., Adriana Szeghalmi., Yong Ye., Jinshi Ma. Mingdao Luo., Ji-ming Hu, and Wolfgang Kiefer, Spectroscopic and computational studies on self-assembly complexes of bis (pyrrol-2-ylmethyleneamine) ligands linked by alkyl spacers with Cu (II), *J. Raman Spectrosc.* 38, 2006, 483 – 495.
- [42] NB. Colthup, LH. Daly, SE. Wiberley. *Introduction to Infrared and Raman Spectroscopy* Academic Press: New York, 1990.
- [43] FR. Dollish, WG. Fateley, FF. Bentley, *Characteristic Raman Frequencies of Organic Compounds* Wiley: New York, 1973.
- [44] G. Socrates, *Infrared Characteristic Group Frequencies* Wiley: New York, 1980.
- [45] LJ. Bellamy, *the Infra-red spectra of Complex Molecules* Wiley: New York, 1975.